



APA 082192

①2 LEVEL III

AD-E 300 688

DNA 5044F

# ATS-6 MEASUREMENTS DURING AVEFRIA

Alan A. Burns  
SRI International  
333 Ravenswood Avenue  
Menlo Park, California 94025

1 August 1979

Final Report for Period 9 January 1978— 15 December 1978

CONTRACT No. DNA 001-78-C-0132

APPROVED FOR PUBLIC RELEASE;  
DISTRIBUTION UNLIMITED.

THIS WORK SPONSORED BY THE DEFENSE NUCLEAR AGENCY  
UNDER RDT&E RMSS CODE B322078462 I25AAXHX63350 H25900.

DDC FILE COPY

Prepared for  
Director  
DEFENSE NUCLEAR AGENCY  
Washington, D. C. 20305

DTIC  
ELECTE  
MAR 25 1980  
S D  
B

Destroy this report when it is no longer  
needed. Do not return to sender.

PLEASE NOTIFY THE DEFENSE NUCLEAR AGENCY,  
ATTN: STTI, WASHINGTON, D.C. 20305, IF  
YOUR ADDRESS IS INCORRECT, IF YOU WISH TO  
BE DELETED FROM THE DISTRIBUTION LIST, OR  
IF THE ADDRESSEE IS NO LONGER EMPLOYED BY  
YOUR ORGANIZATION.



UNCLASSIFIED

SECURITY CLASSIFICATION OF THIS PAGE (When Data Entered)

REPORT DOCUMENTATION PAGE		READ INSTRUCTIONS BEFORE COMPLETING FORM
1. REPORT NUMBER DNA 5044F	2. GOVT ACCESSION NO.	3. RECIPIENT'S CATALOG NUMBER
4. TITLE (and Subtitle) ATS-6 MEASUREMENTS DURING AVEFRIA		5. TYPE OF REPORT & PERIOD COVERED Final Report for Period 9 Jan 78—15 Dec 78
		6. PERFORMING ORG. REPORT NUMBER SRI Project 7107
7. AUTHOR(s) Alan A. Burns		8. CONTRACT OR GRANT NUMBER(s) DNA 001-78-C-0132
9. PERFORMING ORGANIZATION NAME AND ADDRESS SRI International 333 Ravenswood Avenue Menlo Park, California 94025		10. PROGRAM ELEMENT, PROJECT, TASK AREA & WORK UNIT NUMBERS Subtask I25AAXHX633-50
11. CONTROLLING OFFICE NAME AND ADDRESS Director Defense Nuclear Agency Washington, D.C. 20305		12. REPORT DATE 1 August 1979
14. MONITORING AGENCY NAME & ADDRESS (if different from Controlling Office)		13. NUMBER OF PAGES 30
		15. SECURITY CLASS (of this report) UNCLASSIFIED
		15a. DECLASSIFICATION/DOWNGRADING SCHEDULE
16. DISTRIBUTION STATEMENT (of this Report) Approved for public release, distribution unlimited.		
17. DISTRIBUTION STATEMENT (of the abstract entered in Block 20, if different from Report)		
18. SUPPLEMENTARY NOTES This work sponsored by the Defense Nuclear Agency under RDT&E RMSS Code B322078462 I25AAXHX63350 H2590D.		
19. KEY WORDS (Continue on reverse side if necessary and identify by block number) AVEFRIA Barium Ion Clouds RF Propagation Nuclear Weapons Effects Plasma Irregularities		
20. ABSTRACT (Continue on reverse side if necessary and identify by block number) An experimental program was conducted to measure dispersive-phase and amplitude perturbations caused by the AVEFRIA shaped-charge barium release series. 360- and 1550-MHz signals from the ATS-6 geostationary satellite were used for those measurements. A novel technique, whereby the ATS-6 communications subsystem was phase locked to ATS-6 rf beacon, provided a 3950-MHz reference signal for the dispersive phase measurements. Four occultations were achieved during the two AVEFRIA events. Durations of strong effects were		

UNCLASSIFIED

SECURITY CLASSIFICATION OF THIS PAGE (When Data Entered)

20. ABSTRACT (Continued)

as long as four minutes, and some perturbations lasted until T + 20m during one occultation. The greatest amplitude fluctuations measured were +5 to -10 dB at 360 MHz. Maximum estimated phase excursions were about 1 radian at UHF, which corresponds to electron content changes of  $4 \times 10^{10}$  electrons/cm<sup>2</sup>.

→ 10 to the 10<sup>10</sup>  
electrons/cm<sup>2</sup>

UNCLASSIFIED

SECURITY CLASSIFICATION OF THIS PAGE (When Data Entered)

CONTENTS

LIST OF ILLUSTRATIONS . . . . . 2

LIST OF TABLES . . . . . 3

I INTRODUCTION . . . . . 5

II DESCRIPTION OF EXPERIMENT . . . . . 7

    A. Overall Design and Equipment Description . . . . . 7

    B. Geographical Layout . . . . . 13

    C. Operations . . . . . 17

III RESULTS . . . . . 19

IV CONCLUSIONS . . . . . 26

ACCESSION for		
NTIS	White Section	<input checked="" type="checkbox"/>
DOC	Buff Section	<input type="checkbox"/>
UNANNOUNCED		<input type="checkbox"/>
JUSTIFICATION _____		
BY _____		
DISTRIBUTION/AVAILABILITY CODES		
Dist.	AVAIL	and/or SPECIAL
A		

ILLUSTRATIONS

1	ATS-6 Phase Locking Technique . . . . .	8
2	Block Diagram of Additional Ground-Station Equipment . . . . .	10
3	Receiver Front-End Modifications . . . . .	11
4	Ground Station Locations Near Ely, Nevada . . . . .	14
5	Release Locations and Signal Paths . . . . .	16
6	AVEFRIA UNO, White Pine East, UHF and L-Band Amplitude vs Time . . . . .	21
7	AVEFRIA UNO, White Pine West, UHF and L-Band Amplitude vs Time . . . . .	22
8	AVEFRIA DOS, White Pine East, UHF and L-Band Amplitude vs Time . . . . .	23
9	AVEFRIA DOS, White Pine West, UHF and L-Band Amplitude vs Time . . . . .	24
10	WPE--AVEFRIA DOS . . . . .	25

TABLES

1	Link Margin Calculations . . . . .	12
2	Probabilities of Success . . . . .	13
3	Ground Station Locations . . . . .	15
4	Nominal and Actual Release Coordinates . . . . .	15
5	Signal Path Penetration Coordinates . . . . .	15
6	Times After Release of Earliest and Latest Possible Perturbations at UHF . . . . .	20
7	Times After Release of Greatest Activity at UHF . . . . .	20

## I INTRODUCTION

Operation AVEFRIA, which was conducted by the Defense Nuclear Agency (DNA) and the Los Alamos Scientific Laboratory (LASL), consisted of two shaped-charge barium plasma releases into the ionosphere at about 195 km altitude. The releases occurred above the Tonopah Test Range in Nevada on the mornings of 8 and 18 May, 1978. The release times were 1144 and 1135 GMT respectively for AVEFRIA UNO and AVEFRIA DOS.

Although AVEFRIA is the latest in a series of barium-release operations intended to simulate some aspects of high-altitude nuclear effects, particularly those of degradations of satellite communications-command-control functions, the specific AVEFRIA objective was to test the usefulness of the shaped-charge technique. It was expected that the shaped-charge barium plasma injection method would provide a promptly striated ion cloud, which would allow use of fixed ground stations rather than expensive airborne platforms for rf propagation experiments. Operation AVEFRIA very successfully proved these expectations.

The efforts reported here involved fixed ground-based measurements, which used signals from the ATS-6 geostationary satellite. Amplitude-perturbation and dispersive-phase-perturbation measurements were made at 360 and 1550 MHz. The reference frequency for the dispersive-phase measurements was 3950 MHz, the amplitude of which was recorded. A novel technique was used to phase-lock the 360 MHz ATS-6 beacon signal to the 1550- and 3950-MHz signals, which eliminated any unknown fluctuations inherent in the master oscillator for the 360-MHz signal on board the spacecraft. By using such high measurement and reference frequencies, the measurement-distorting effects caused by scattering and diffraction were greatly reduced, and in most cases eliminated entirely. This experiment was also very successful.

Because this contract called for an assessment of the quantity and quality of any data collected, only quick-look data analysis has been

carried out. These show that rather long duration occultations were obtained, and, in one case, the effects lasted almost twenty minutes. Since occultations were achieved at both stations on the two AVEFRIA events, four occultations were obtained overall. As expected from the choice of high operating and reference frequencies and the small amount of barium, rf effects were generally very small. Fades at UHF rarely exceeded 5 dB, and amplitude fluctuations always remained within -15 and +5 dB of the unperturbed signal level. Amplitude fluctuations at L-band were much smaller than that, of course.

The first part of this report is a description of the experiment. That is followed by a presentation of some of the results.

## II DESCRIPTION OF THE EXPERIMENT

### A. Overall Design and Equipment

The standard dispersive phase technique was used to make these measurements. They were accomplished, however, in an innovative way because a much higher frequency reference signal was provided using a novel technique. The new technique was to lock the 6.15-GHz PLACE uplink signal to the 360-MHz beacon signal received at a ground station where scintillation activity would be usually weak or nonexistent. Figure 1 depicts the arrangement.

As designed for the PLACE experiment, the ATS-6 transponder can be operated in a phase-locked mode in which signals at 1.55 and 3.75 GHz coherent with the  $6.15 \pm 0.012$  GHz uplink signal are transmitted from the satellite. The frequencies of the 1.55- and 3.75-GHz signals are related to that of the 6.15-GHz signal by the factors  $31/(3 \times 41)$  and  $25/41$ , respectively. Thus, a particularly good choice for the multiplication factor at the reference ground station between the received 360.144-MHz downlink beacon signal and the locally synthesized 6.15-GHz uplink signal was  $12/(5 \times 41)$  because it led to a relatively convenient ratio of 12/125 between the 360-MHz and 3.75-GHz downlink signals.

Standard dispersive-phase measurements can be made at any measurement ground station using the 3.75-GHz downlink signal as the reference. The measured phase, however, includes substantial phase shifts because of the two-way path between the satellite and the reference ground station. Suppose that the dispersive phase along that path follows the  $1/f$  dependence expected for undisturbed ionospheric conditions and is equal to  $\Delta\phi_{360}$  at 360 MHz. Then, if the path is  $d$  meters long, the phase difference referred to 360 MHz between the 360-MHz beacon signal and the 3.75-GHz transponder signal is given by

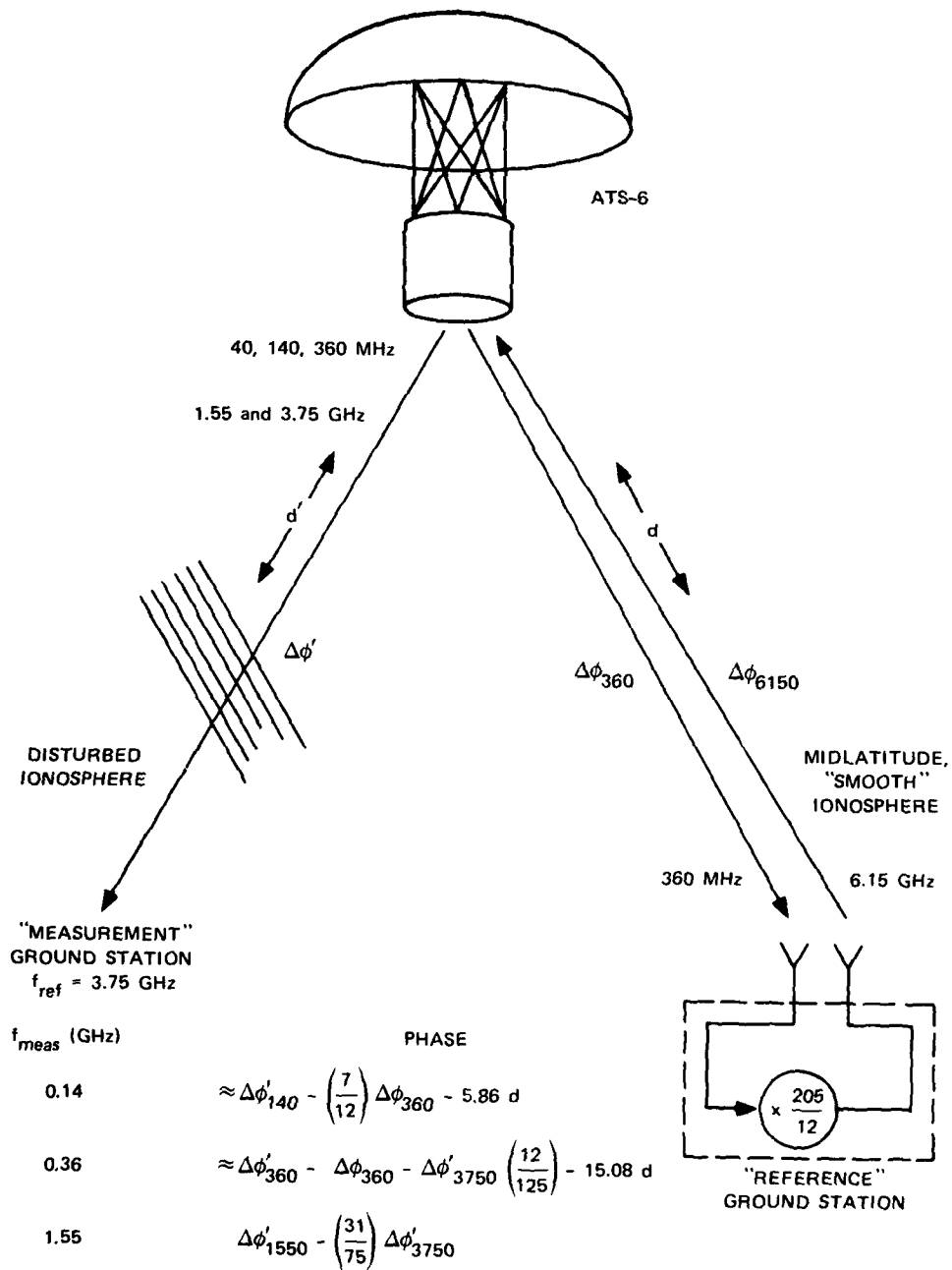


FIGURE 1 ATS-6 PHASE LOCKING TECHNIQUE

$$\begin{aligned}
\varphi_e &= \Delta\varphi_{360} + \left(\frac{360}{6150}\right) \Delta\varphi_{6150} + 2k_{360}d \\
&= \Delta\varphi_{360} \left[1 + \left(\frac{360}{6150}\right)\right]^2 + 4 \frac{3.6 \times 10^8}{3 \times 10^8} d \\
&\cong \Delta\varphi_{360} + 15.08d \quad .
\end{aligned}$$

Thus, if the dispersive phases along the measurement path are  $\Delta\varphi'_{360}$  and  $\Delta\varphi'_{3750}$ , the phase measurement would yield

$$\varphi \cong \Delta\varphi'_{360} - \Delta\varphi'_{3750} - \Delta\varphi_{360} - 15.08d \quad .$$

Because  $d$  changes very slowly for a geostationary satellite and because  $\Delta\varphi_{360}$  was slowly varying as well, this technique provided a good measurement of phase changes caused by disturbed conditions along the measurement path. Such changes were much more important than the total phase shift for the AVEFRIA operation.

The most cost-effective choice for the reference ground station was to use the single remaining ATS-6 ground station at Rosman, N.C. Because the satellite was only about  $12^\circ$  above the horizon at Rosman, there was some concern that the fairly long transionospheric path might cause a problem. No difficulties, however, were experienced. Figure 2 shows a block diagram of the additional equipment installed at Rosman. An existing antenna was made available for this experiment. The amplitude and phase of the downlink signal was monitored and recorded, but no anomalies occurred during the tests (local thunderstorm activity caused some drop-outs on a non-test day).

To keep hardware costs for this experiment down, the SRI project staff determined that the ground station receivers could readily be built using DNA-owned receivers built for the SECEDE program by Electrac, Inc., and available at SRI International. These receivers use tracking filters and were designed to measure relative amplitudes and differential phase

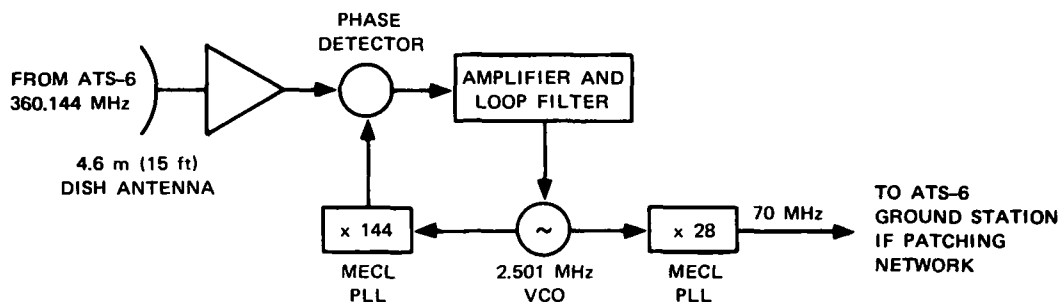


FIGURE 2 BLOCK DIAGRAM OF ADDITIONAL GROUND-STATION EQUIPMENT (required for phase locking the ATS-6 communications subsystem to the ATS-6 radio beacon experiment signal)

of four coherent signals at 145.7644 MHz, 291.5288 MHz, 437.2932 MHz, and 874.5864 MHz. They were used for the present experiment by down-converting each ATS-6 signal to one of these four frequencies.

The approach used to implement these conversions is presented in Figure 3. The design shown in this figure permits the use of the Electrac receivers in their present configuration. The only additional hardware necessary are readily available items and hardware already designed and tested at SRI on previous projects.

The design of the ground station was an open-loop configuration in which no phase-locked loop is used to stabilize the HP-105 oscillator. However, the short-term frequency stability of this oscillator ( $1 \times 10^{-11}$  for 10 s, 1s and  $10^{-1}$  s; and  $1 \times 10^{-10}$  for  $10^{-2}$  s) was sufficient to permit the collection and interpretation of data on phase perturbations induced in the UHF and L-band signals by the ionosphere.

Table 1 presents the link calculations for the measurement link. The following antennas were used:

- (1) 360-MHz channel; 3m (10 ft) dish
- (2) 1550-MHz channel; 1.8m (6 ft) dish
- (3) 3751-MHz channel; 1.2m (4 ft) dish.

The link SNRs were quite adequate for this application.

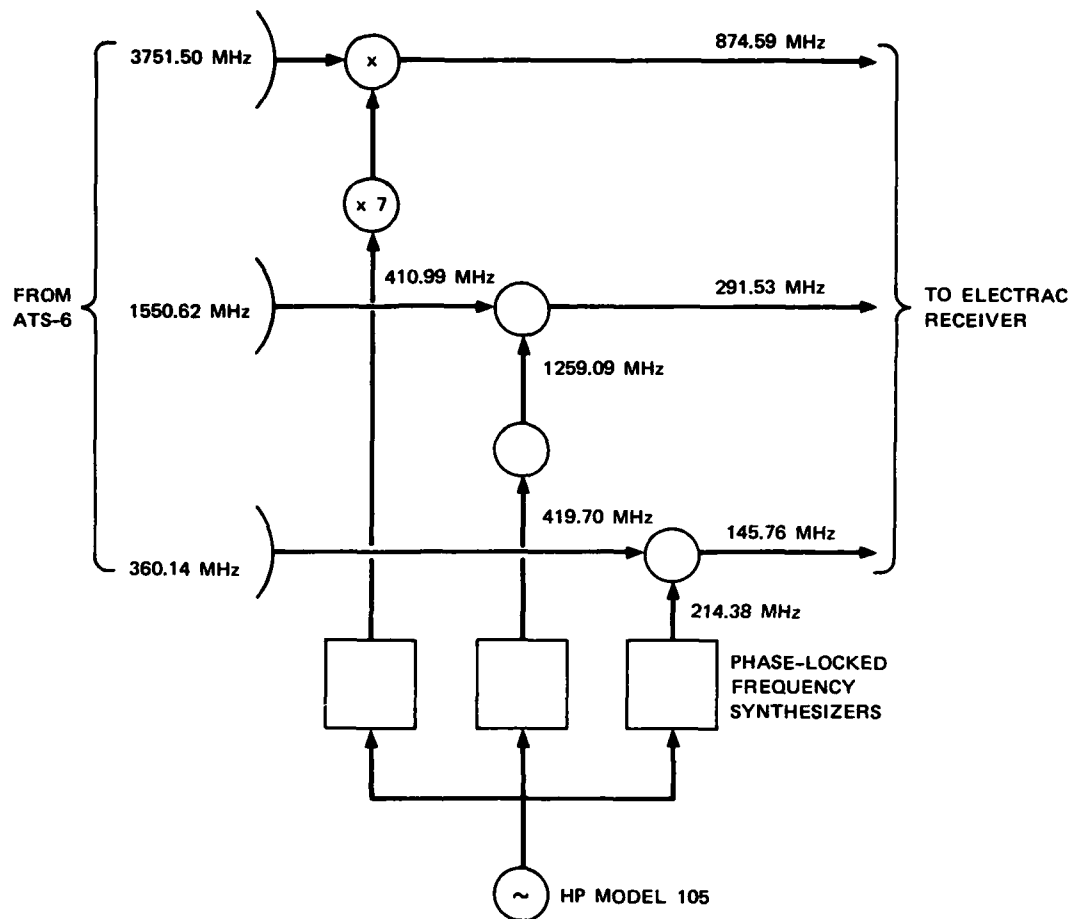


FIGURE 3 RECEIVER FRONT-END MODIFICATIONS

Analog data recording was used. The amplitude and pair of phase signals at 360 and 1550 MHz were individually recorded on six separate tracks of an FM tape recorder. In addition, the 3650-MHz reference signal amplitude and a 10-kHz IRIG time code signal were multiplexed onto the seventh channel. One of the phase signals from each of the measurement signals were recorded in real time with a strip-chart recorder. Although the strip chart recorder was provided primarily for monitoring the experiment, it also acted as a backup in case of primary recorder failure.

Table 1  
LINK MARGIN CALCULATIONS

Channel	Frequency (MHz)	EIRP* (dBW)	Free Space Path Loss ( $1/4\pi R$ )† (dB)	Cable Loss (dB)	Margin (dB)	Antenna‡ Gain (dB)	Received Power (dBW)	Preamplifier Noise Figure (dB)	Antenna Temperature (K)	Cable Loss (dB)	System Temperature (K)	Receiver** Bandwidth (Hz)	Boltzman's Constant (W/Hz/K)	Effective Noise Power (dBW)	SNR (dB)
1	360	3	-176	-2	-3	18.5	-159.5	4	$3 \times 10^3$	2	$2.4 \times 10^3$	50	$1.4 \times 10^{-23}$	-178	18.5
2	1550	42	-189	-4	-3	26	-128	3	300	4	600	50	$1.4 \times 10^{-23}$	-184	56
3	3751	24	-196	-4	-3	31	-148	4	300	4	738	50	$1.4 \times 10^{-23}$	-183	35

\* Data taken from "ATS-6 Mission Design--Orbital Performance, Revision 1," Fairchild Industries (October 1975).

† In the expression,  $R$  = range,  $\lambda$  = wavelength.

‡ An antenna efficiency of 55% is assumed.

\*\* Referenced to input of preamplifier.

\*\* Receiver bandwidth chosen commensurate with experiment objectives and options available on Electrac receivers.

B. Geographical Layout

A simple analysis involving rocket dispersion parameters to determine the probabilities of achieving occultations indicated that while two ground stations were much better than one, adding a third station was not justified. Table 2 presents the results of that analysis; shown are the probabilities,  $P_{n/m}$ , of  $n$  successes in  $m$  times of the actual release point being within 3.5 and 5 km of a line of sight. Because the barium injection was to be toward the east and the cloud was expected to drift west, the two stations were aligned in roughly an east-west direction. Figure 4 is a map of the station locations, which were in the vicinity of Ely, Nevada. They were named White Pine East (WEP) and White Pine West (WPW), after the county they were in. Table 3 lists the station coordinates. The Los Alamos Scientific Laboratory colocated one of their optical stations with each of the two SRI receiver sites.

Table 2  
PROBABILITIES OF SUCCESS

	Distance from Release Point (km)					
	≤ 3.5			≤ 5		
	$P_1$	$P_{1/2}$	$P_{2/2}$	$P_1$	$P_{1/2}$	$P_{2/2}$
1 Station	0.68	0.90	0.46	0.85	0.98	0.72
2 Stations	0.87	0.98	0.76	0.97	0.999	0.94
3 Stations	0.95	0.998	0.91	0.996	≈ 1	0.992

Figure 5 shows the spatial relationship among the receiving stations, the nominal release point at 195-km altitude, the actual release points, and the points where the signal paths from ATS-6 penetrated the altitudes at which the barium releases actually occurred. Both releases occurred well to the east of the nominal location, but the westward drifts of the clouds ensured that four occultations were achieved. Table 4 lists the nominal and actual release positions, and Table 5 shows the coordinates

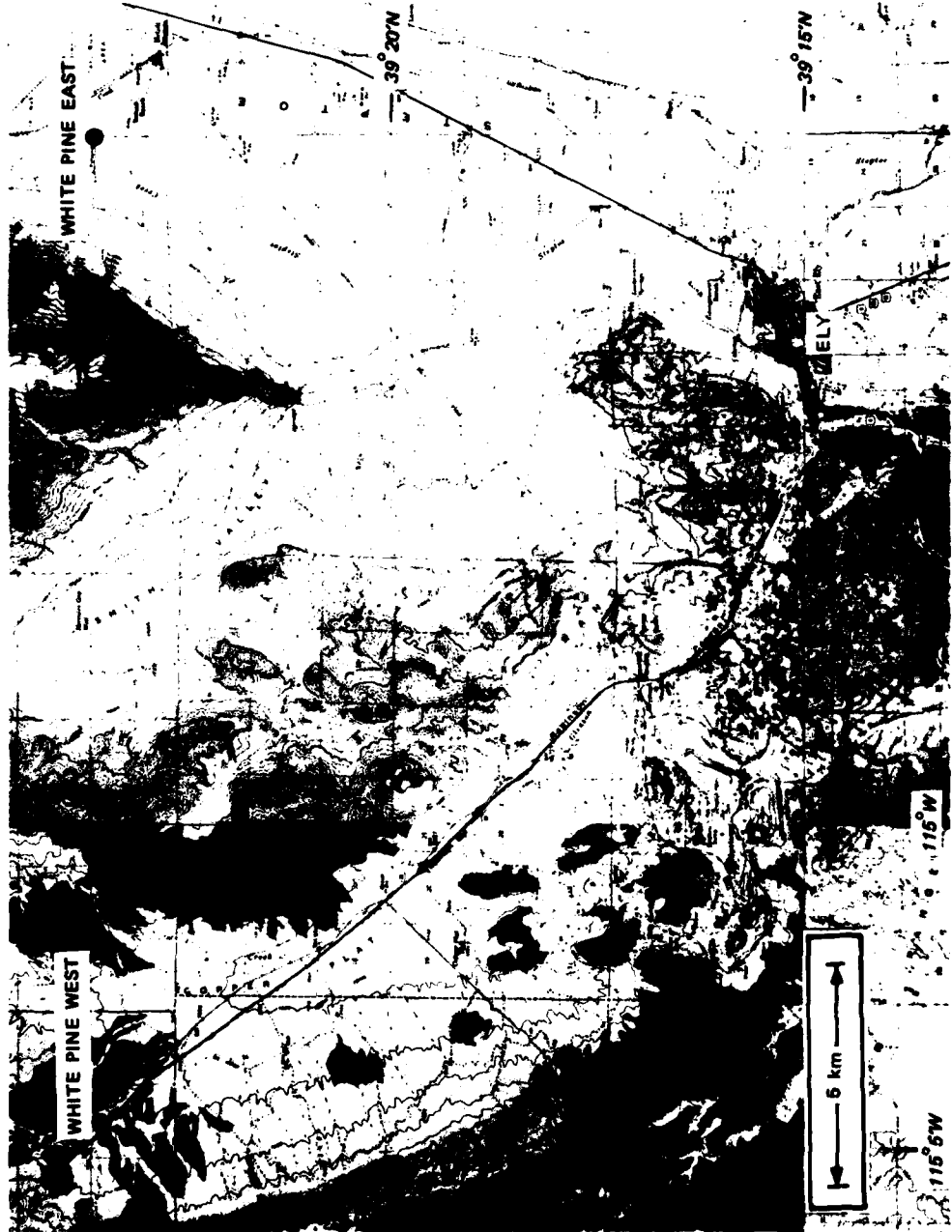


FIGURE 4 GROUND STATION LOCATIONS NEAR ELY, NEVADA

Table 3

## GROUND STATION LOCATIONS

Station	Altitude (m)	N Latitude	W Longitude
White Pine East	1829	39.39.167	114.82479
White Pine West	2178	39.39045	115.07623

Table 4

## NOMINAL AND ACTUAL RELEASE COORDINATES

Event	Altitude (km)	N Latitude	W Longitude
Nominal	195.0	37.650	116.54
Uno	193.1	37.617	116.394
Dos	190.1	37.700	116.325

Table 5

## SIGNAL PATH PENETRATION COORDINATES

Event	Ground Station	Altitude (km)	N Latitude	W Longitude
Uno	WPE	193.1	37.687	116.419
	WPW		37.689	116.649
Dos	WPE	190.1	37.695	116.406
	WPW		37.698	116.636

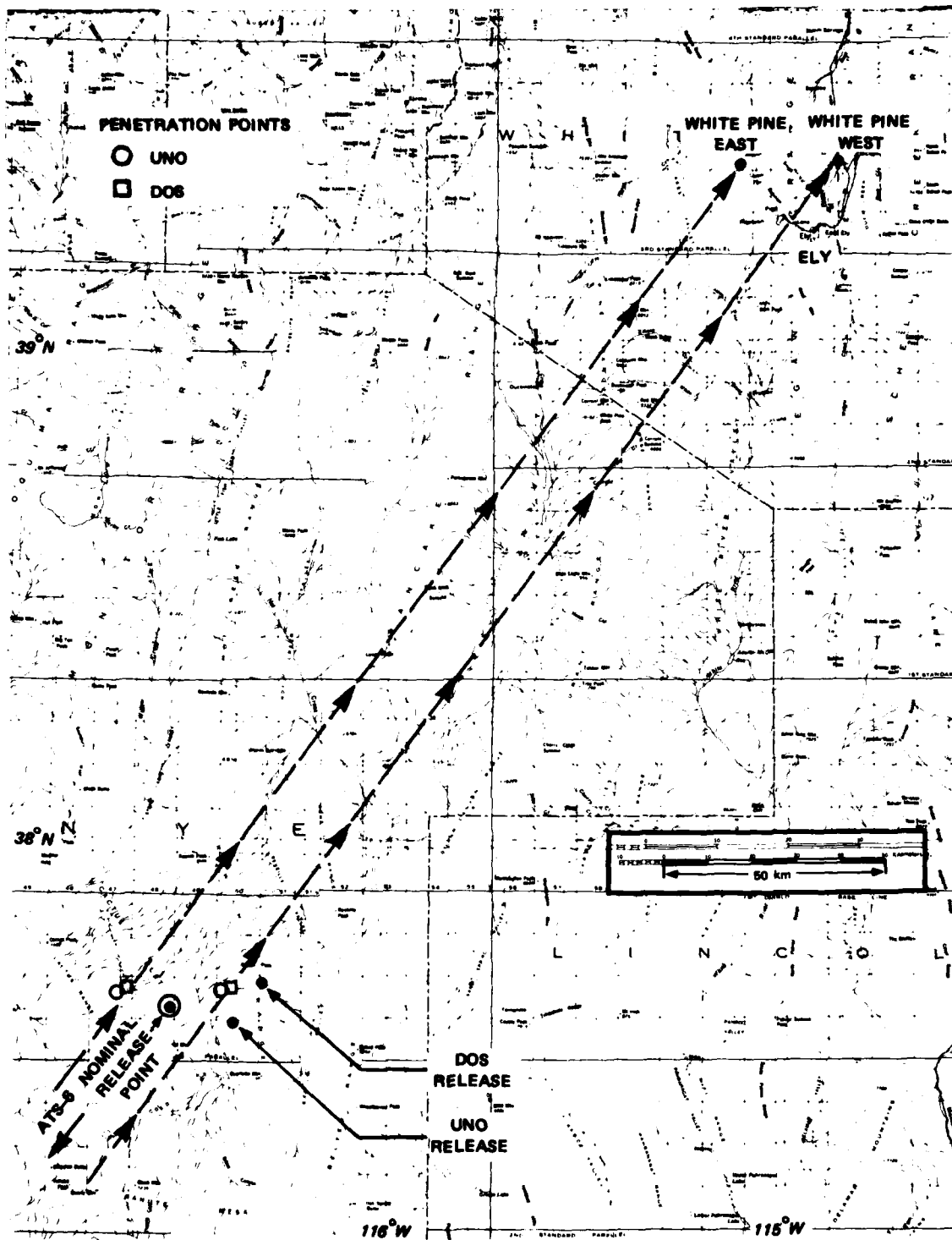


FIGURE 5 RELEASE LOCATIONS AND SIGNAL PATHS

of the ATS-6 signal path penetration points.\* The angles between the geomagnetic field and the signal paths at the release altitudes were about 26.5°.

### C. Operations

The equipment was fielded according to schedule and was entirely operational by the first day in the launch window. Some minor problems were encountered because of lower-than-anticipated temperatures. These were solved by installing a larger generator at one site and a sufficient number of heaters to keep the equipment warm.

A schedule was established with the NASA ATS-6 operations office, whereby several hours of time were reserved for the AVEFRIA operation on potential event days. Approximately one and one-half hours before an event the attitude of the ATS-6 satellite was shifted to point its antennas toward the ground station. This move was necessary because of the narrow beamwidth of the L-band antenna on the spacecraft. Then the proper subsystems were activated, phase lock was established, and the L-band transmitter was turned on. Although the duration of operation was, in principle, limited by the large power drain of the ATS-6 L-band transmitter, that was not a factor for this AVEFRIA experiment.

Amplitude calibrations were made by means of variable attenuators between the preamplifier/downconverter systems and the main part of the receivers. Calibrations were carried out both immediately preceding the events and after all possible effects had ceased. There were no phase calibrations per se; that information can be recovered from the data itself using a histogram technique.

It was noticed that the Doppler shift caused by satellite motion and total electron content changes along both the measurement and phase-locking signal paths varied in regular and predictable ways. Thus,

---

\*AVEFRIA location data were generated by J. Clynch of the Applied Research Laboratories, University of Texas. The latitudes are geodetic and altitudes are referenced to the geoid.

before the events the Doppler offsets were set by the operators to small values so that zero offset would be reached several minutes later. The idea was to reach zero Doppler shift during the expected middle of the occultation period. The phase-locked frequency synthesizers permitted setting the Doppler offsets to a small fraction of a cycle per second.

### III RESULTS

Discernible amplitude fluctuations spanned fairly long time intervals during both events. However, the perturbations were generally quite episodic, apparently resulting from particles of structured ionization or striations passing through the signal paths. Table 6 presents the earliest and latest times after release of amplitude fluctuations seen at 360 MHz that may have been due to the releases. Table 7 shows the time spans of greatest 360-MHz signal fluctuation and semi-quantitative estimates of the fluctuations that occurred during those times. Large, isolated perturbations of brief duration happened at other times as well.

Figures 6 through 9 show strip-chart recordings of the 360- and 1550-MHz amplitude fluctuations during the periods of maximum perturbation. There are significant differences between the natures of the perturbations measured at different stations even on the same event. The differences are due to temporal or spatial differences in the structure of the ionization causing the perturbations. By far the largest effects occurred on the WPE AVEFRIA DOS occultation.

As expected, the L-band amplitudes were only slightly perturbed. This is an indication that no appreciable phase shift (i.e.,  $< 1$  rad) took place within the distance of one Fresnel zone at 1550 MHz. At that frequency the radius of the first Fresnel zone was about 365 m. In contrast, the 360-MHz Fresnel zone radius was about 755 m.

Figure 10 shows a portion of the amplitude and one of the quadrature phase signals at 360 and 1550 MHz for the WPE AVEFRIA DOS occultation. Even though the UHF Doppler offset was only 0.6 Hz, it is very difficult to isolate cloud-induced phase shifts in this type of a record--the trend must be subtracted first. Nevertheless, it appears that phase shifts at UHF were not much greater than one radian. We note that an integrated electron density (electron content) of  $4.2 \times 10^{10}$  el/cm<sup>2</sup> is required to

Table 6

TIMES AFTER RELEASE OF EARLIEST  
AND LATEST POSSIBLE PERTURBATIONS AT UHF

Event	Station	Greatest Extent of Times of Possible Perturbation	
		Earliest	Latest
UNO	WPE	T + 2m 53s	T + 5m 53s
	WPW	T + 1m 27s	T + 10m 27s
DOS	WPE	T + 2m 28s	T + 7m 44s
	WPW	T + 0m 05s	T + 19 m 40s

Table 7

TIMES AFTER RELEASE OF GREATEST  
ACTIVITY AT UHF

Event	Station	Time Span	Amplitude Fluctuation
UNO	WPE	2m 53s - 3m 54s	+1, -3 dB
	WPW	3m 40s - 7m 42s	+3, -5 dB
DOS	WPE	2m 30s - 5m	+5, -10 dB
	WPW	8m 30s - 9m 25s	+1, -3 dB
	WPW	10 m 08s - 12m 58s	+1, -3 dB

produce one radian of phase shift at 360 MHz. The corresponding phase shift at 1550 MHz is about 13 degrees. The more rapid fluctuations that can be seen in the 1550-MHz phase record in Figure 10 appear to be somewhat smaller than that value.

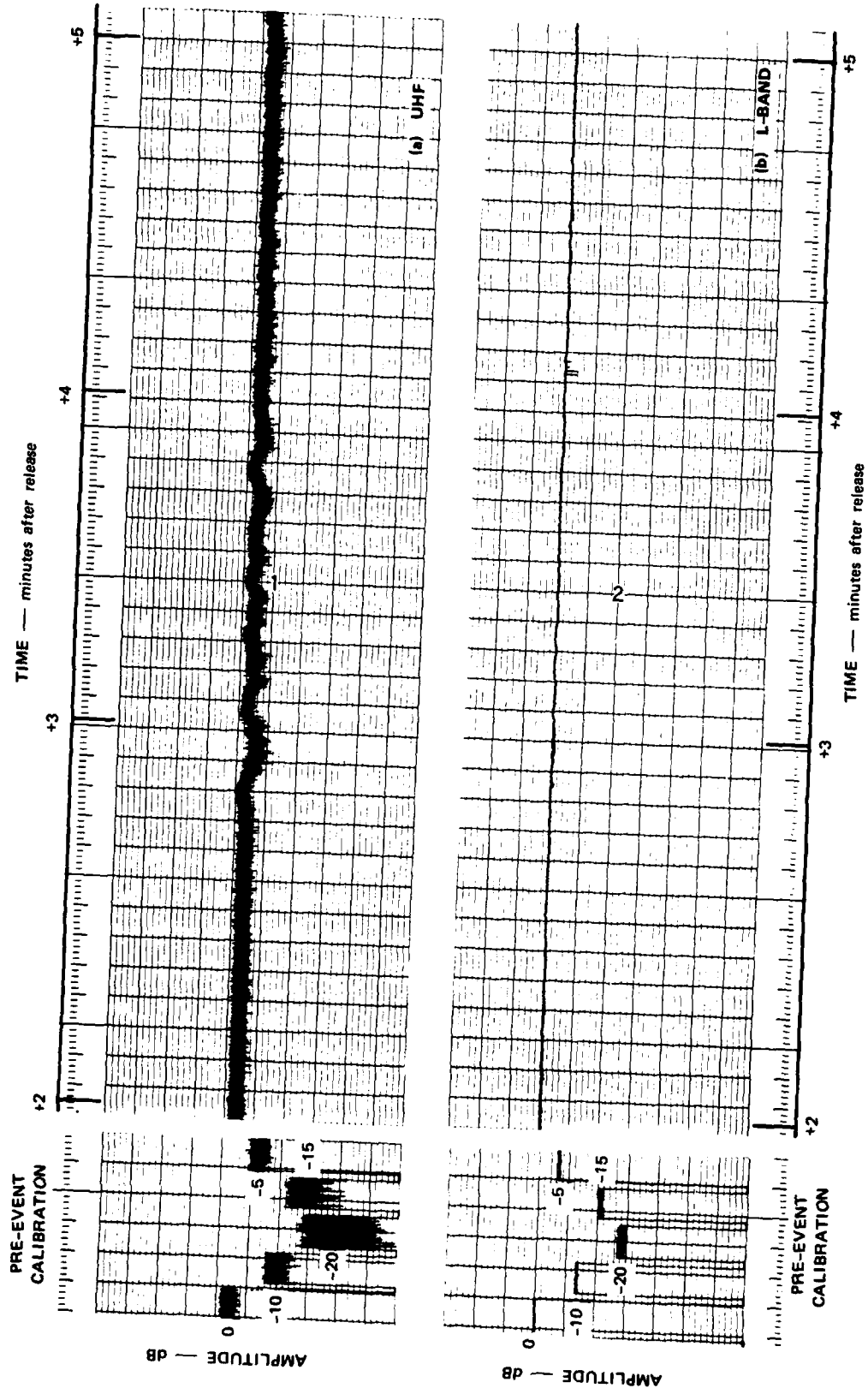


FIGURE 6 AVEFRIA UNO, WHITE PINE EAST, UHF AND L-BAND AMPLITUDE vs. TIME

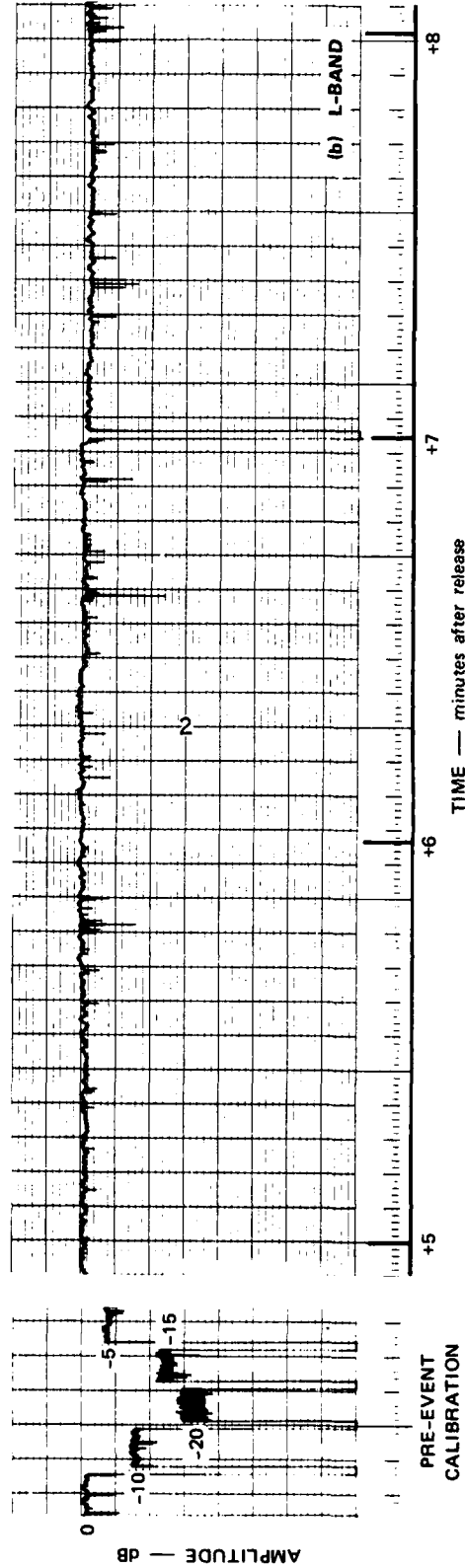
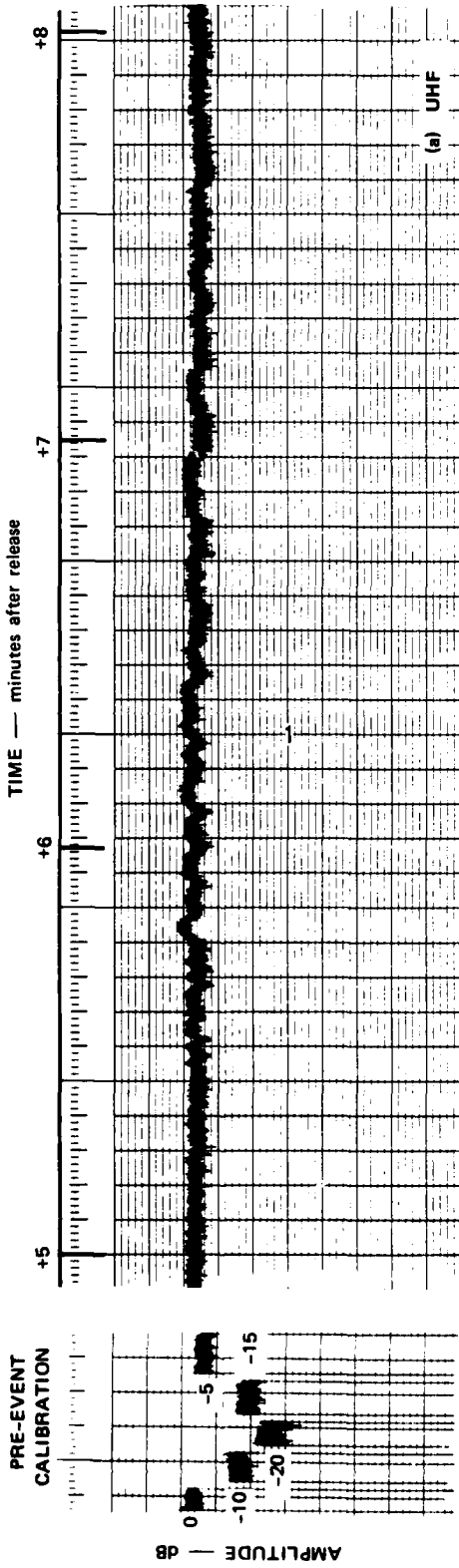


FIGURE 7 AVEFRIA UNO, WHITE PINE WEST, UHF AND L-BAND AMPLITUDE vs. TIME

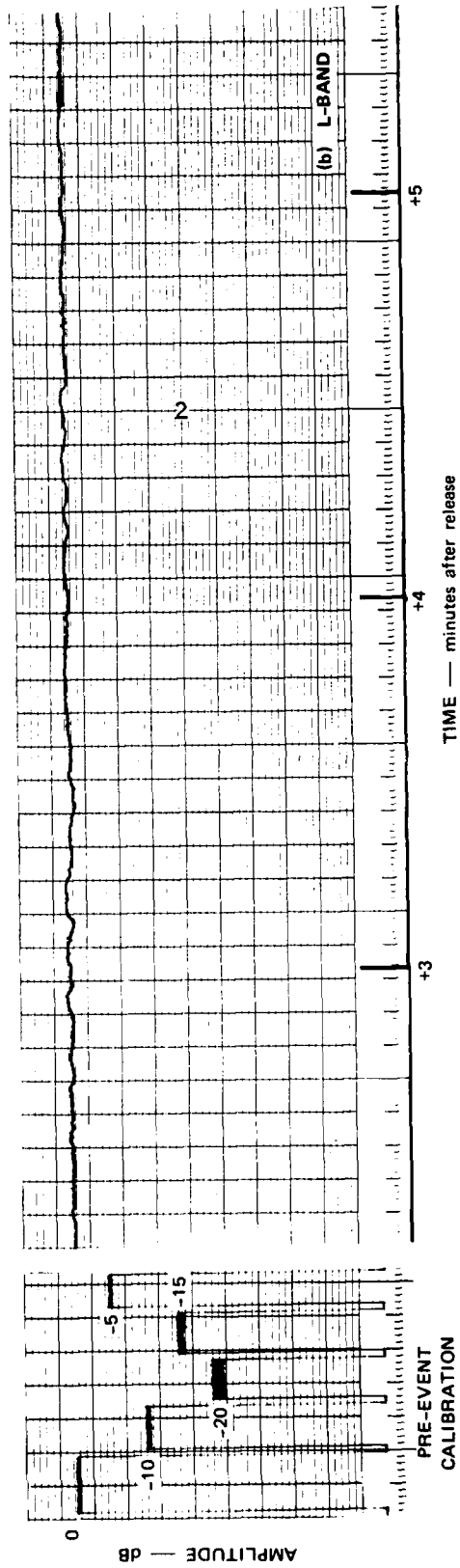
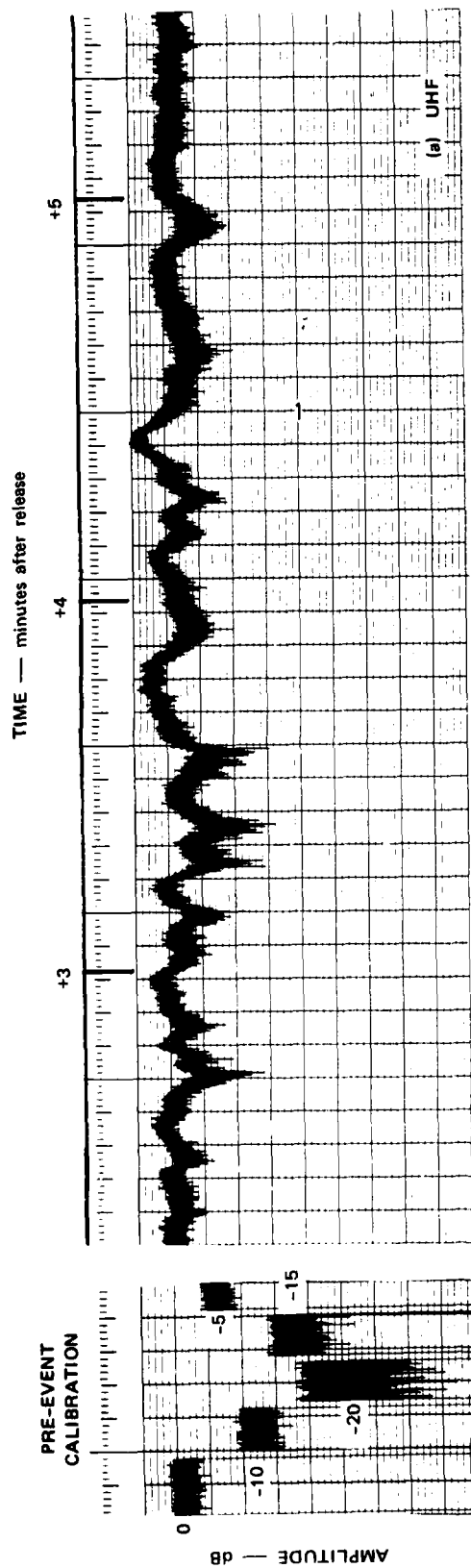


FIGURE 8 AVEFRIA DOS, WHITE PINE EAST, UHF AND L-BAND AMPLITUDE vs. TIME

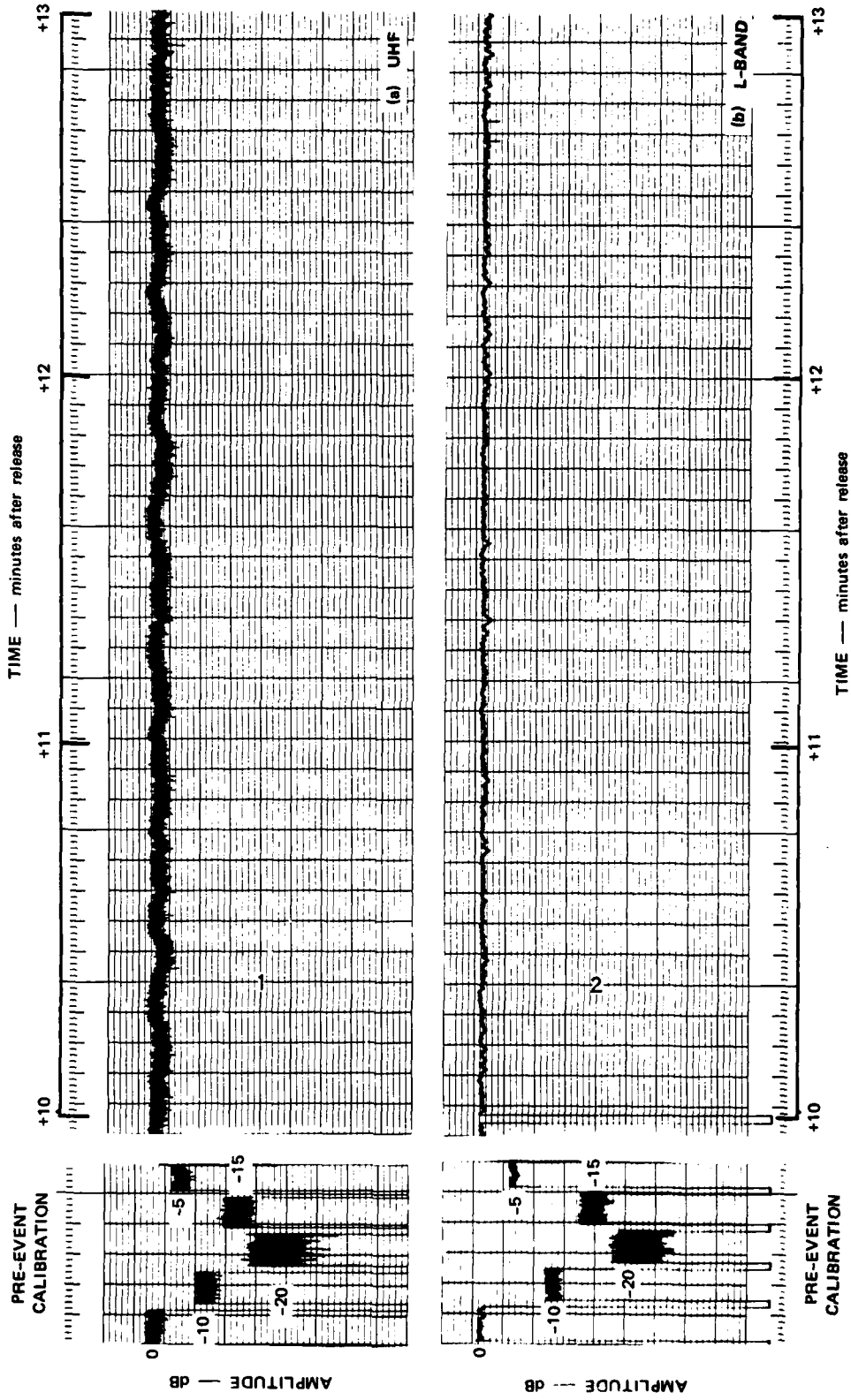


FIGURE 9 AVEFRIA DOS, WHITE PINE WEST, UHF AND L-BAND AMPLITUDE VS. TIME

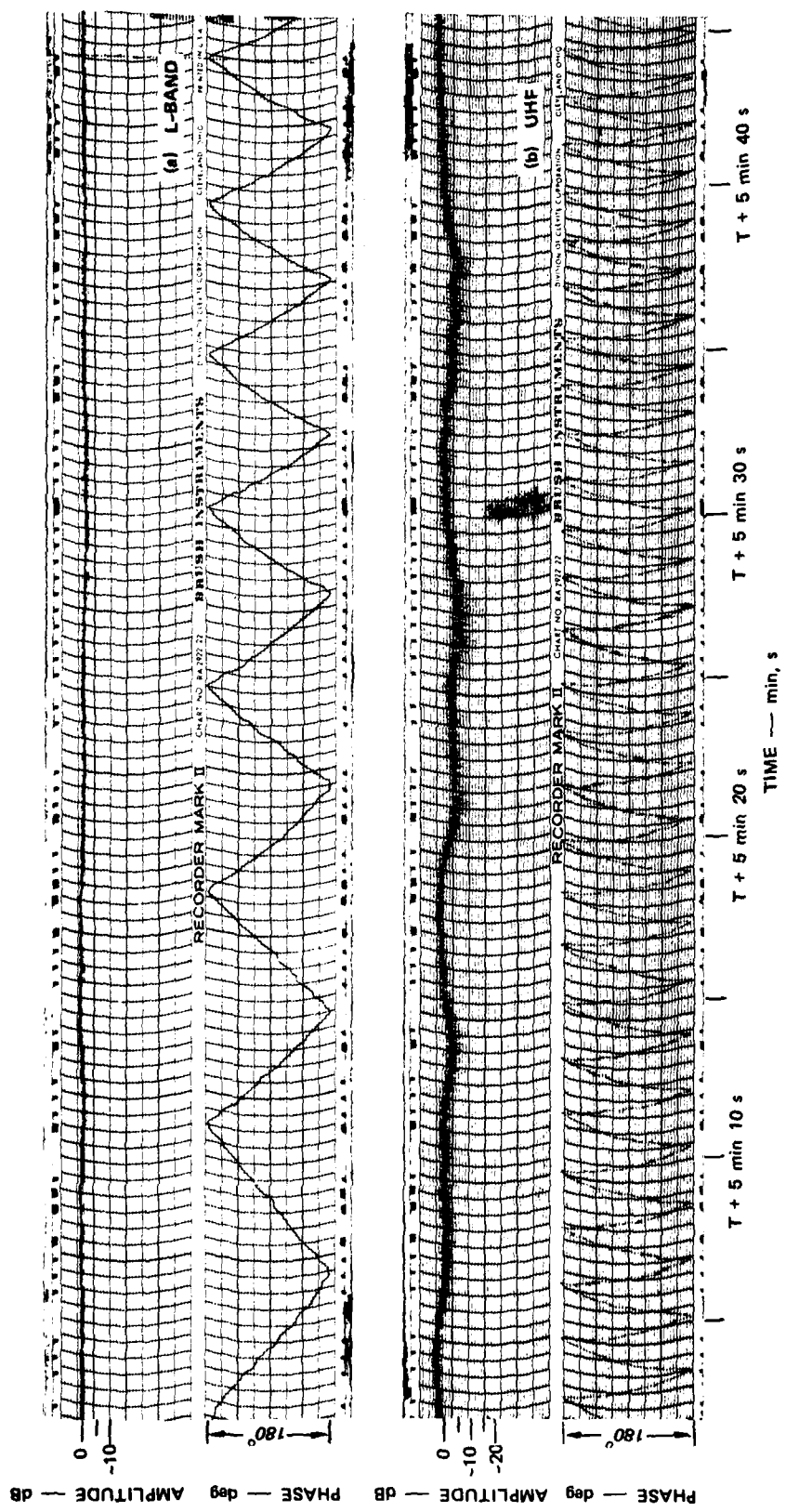


FIGURE 10 AVEFRIA DOS, WHITE PINE EAST

#### IV CONCLUSIONS

Four occultations of varying durations and intensities of effects were achieved. The strongest effects were +5 to -10 amplitude fluctuations and phase perturbations on the order of one radian. That corresponds to electron content changes of several times  $10^{10}$  electrons per square centimeter.

Only quick-look data results could be reported here. Detrending the phase data to isolate perturbations due to the AVEFRIA ion-cloud, would constitute the major part of any future data reduction effort. The data have been digitized already. Comparisons should then be made with data collected by the Los Alamos Scientific Laboratory, which installed image-intensified optics at collocated ground stations. The overall objective would be to derive spatial frequency spectra of the shaped-charge AVEFRIA barium releases.

In general, the ATS-6 experiment was quite successful. All of the equipment worked normally. It was demonstrated that the ATS-6 communications subsystem could be phase locked to its beacon transmitter. This provided a very high frequency (3950 MHz) reference signal for dispersive phase measurements.

## DISTRIBUTION LIST

### DEPARTMENT OF DEFENSE

Assistant to the Secretary of Defense  
Atomic Energy

ATTN: Executive Assistant

Defense Advanced Rsch. Proj. Agency

ATTN: TIO

Defense Communications Engineer Center

ATTN: Code R123

Defense Nuclear Agency

ATTN: DDST

ATTN: STVL

3 cy ATTN: RAAE

4 cy ATTN: TITL

Defense Technical Information Center

12 cy ATTN: DD

Field Command

Defense Nuclear Agency

ATTN: FCPR

Field Command

Defense Nuclear Agency

Livermore Division

ATTN: FCPRL

Undersecretary of Def. for Rsch. & Engrg.

ATTN: Strategic & Space Systems (OS)

### DEPARTMENT OF THE ARMY

Harry Diamond Laboratories

Department of the Army

ATTN: DELHD-N-P

U.S. Army Nuclear & Chemical Agency

ATTN: Library

### DEPARTMENT OF THE NAVY

Naval Ocean Systems Center

ATTN: Code 5322, M. Paulson

Naval Research Laboratory

ATTN: Code 6700, T. Coffey

ATTN: Code 6780, S. Ossakow

Naval Surface Weapons Center

ATTN: Code F31

Strategic Systems Project Office

Department of the Navy

ATTN: NSP-43

### DEPARTMENT OF THE AIR FORCE

Air Force Geophysics Laboratory

ATTN: OPR-1, J. Ulwick

ATTN: PHP, J. Aarons

ATTN: PHP, J. Mullen

### DEPARTMENT OF THE AIR FORCE (Continued)

Air Force Weapons Laboratory

Air Force Systems Command

ATTN: SUL

ATTN: DYC

Headquarters

Electronic Systems Division

ATTN: DCKC, J. Clark

### DEPARTMENT OF ENERGY

Lawrence Livermore Laboratory

ATTN: Document Control for Tech. Info.  
Dept. Lib.

Los Alamos Scientific Laboratory

ATTN: Document Control for D. Simons

### DEPARTMENT OF DEFENSE CONTRACTORS

Berkeley Research Associates, Inc.

ATTN: J. Workman

ESL, Inc.

ATTN: J. Marshall

ATTN: C. Prettie

ATTN: J. Roberts

General Electric Company-TEMPO

ATTN: W. Knapp

ATTN: DASIAC

General Research Corp.

ATTN: J. Garbarino

ATTN: J. Ise, Jr.

GTE Sylvania, Inc.

Electronics Systems Group

ATTN: M. Cross

University of Illinois

ATTN: Security Supervisor for K. Yeh

JAYCOR

ATTN: S. Goldman

M.I.T. Lincoln Lab

ATTN: D. Towle

Mission Research Corp.

ATTN: R. Bogusch

ATTN: R. Kilb

ATTN: D. Sappenfield

Physical Dynamics, Inc.

ATTN: E. Fremouw

R & D Associates

ATTN: B. Gabbard

ATTN: R. Lelevier

ATTN: C. MacDonald

DEPARTMENT OF DEFENSE CONTRACTORS (Continued)

R & D Associates

ATTN: B. Yoon

Rand Corp.

ATTN: E. Bedrozian

Science Applications, Inc.

ATTN: D. Sachs

ATTN: L. Linson

Utah State University

Space Measurements Lab

ATTN: L. Jensen

ATTN: K. Baker

DEPARTMENT OF DEFENSE CONTRACTORS (Continued)

SRI International

ATTN: M. Baron

ATTN: W. Chesnut

ATTN: C. Rino

ATTN: A. Burns

Technology International Corp.

ATTN: W. Boquist